

Intensity Distribution Function and Statistical Properties of Fast Radio Bursts

Long-Biao Li^{1,2}, Yong-Feng Huang^{1,2*}, Zhi-Bin Zhang³, Di Li^{4,5}, Bing Li^{1,6}

¹ School of Astronomy and Space Science, Nanjing University, Nanjing 210046, China

² Key Laboratory of Modern Astronomy and Astrophysics (Nanjing University), Ministry of Education, Nanjing 210046, China

³ Department of Physics, College of Sciences, Guizhou University, Guiyang 550025, China

⁴ National Astronomical Observatories, Chinese Academy of Sciences, Beijing 100012, China

⁵ Key Laboratory for Radio Astronomy, Chinese Academy of Sciences, China

⁶ Institute of High Energy Physics, Chinese Academy of Sciences, Beijing 100049, China

26 April 2019

ABSTRACT

Fast Radio Bursts (FRBs) are intense radio flashes from the sky that are characterized by millisecond durations and Jansky-level flux densities. We carry out a statistical analysis on FRBs discovered. Their mean dispersion measure, after subtracting the contribution from the interstellar medium of our Galaxy, is found to be $\sim 658 \text{ pc cm}^{-3}$, supporting the idea that they are of cosmological origin. Their energy released in radio band spans about three orders of magnitude, with a mean value of $\sim 10^{39} \text{ ergs}$. More interestingly, although the FRB study is still in a very early phase, the already considerable number of FRBs enables us to derive a useful intensity distribution function. For the 16 non-repeating FRBs detected by Parkes telescope and the Green Bank Hydrogen Telescope, the function can be derived as $dN/dF_{\text{obs}} = (4.14 \pm 1.30) \times 10^3 F_{\text{obs}}^{-1.14 \pm 0.20} \text{ sky}^{-1} \text{ day}^{-1}$, where F_{obs} is the observed radio fluence in units of Jy ms. Based on this intensity distribution function, it is estimated that the Chinese Five-hundred-meter Aperture Spherical radio Telescope will be able to detect about 5 FRBs for every 1000 hours of observation time. Additionally, if we include all the repeating events from the direction of FRB 121102 in the analysis, then the power-law index becomes 1.95 ± 0.29 , more approaching the expected value of 2.5 for standard candles distributed homogeneously in a flat Euclidean space.

Key words: pulsars: general – stars: neutron – radio continuum: general – intergalactic medium – methods: statistical

1 INTRODUCTION

Fast Radio Bursts (FRBs) are intense radio flashes that occur randomly in the sky. They are characterized by their strong brightness ($\geq 1 \text{ Jy}$), but with very short durations ($\sim \text{ms}$). Until March 2016, 16 non-repeating bursts and 17 repeating bursts have been discovered as the originally unexpected outcomes of fast radio transient surveys (Lorimer et al. 2007; Keane et al. 2012; Thornton et al. 2013; Burke-Spolaor & Bannister 2014; Spitler et al. 2014; Champion et al. 2016; Masui et al. 2015; Petroff et al. 2015a; Ravi, Shannon & Jameson 2015; Keane et al. 2016; Scholz et al. 2016; Spitler et al. 2016). Except for the unique detection of radio afterglow and host galaxy of FRB 150418 (Keane et al. 2016), most previous efforts trying to search

for the counterparts of other FRBs have led to a negative result (e.g. Petroff et al. 2015a). Very recently, Spitler et al. (2016) and Scholz et al. (2016) discovered sixteen repeating bursts from the direction of FRB 121102, providing valuable clues on the nature of these enigma events (Dai et al. 2016; Gu et al. 2016). Note that although FRB 140514 has been detected in almost the same direction of FRB 110220, it is considered to be a separate event because of its different dispersion measure (DM) (Petroff et al. 2015b).

The arrival time of an FRB at different wavelength is characterized by a frequency-dependent delay of $\Delta t \propto \nu^{-2}$, and the pulse width is found to scale as $W_{\text{obs}} \propto \nu^{-4}$ (Lorimer et al. 2007; Thornton et al. 2013). Both characteristics are consistent with the expectations for radio pulses propagating through a cold, ionized plasma. These facts strengthen the view that FRBs are of astrophysical origin. The dispersion measure, defined as the line-of-sight integral

* E-mail: hyf@nju.edu.cn

of the free electron number density, is a useful indication for distance. An outstanding feature of FRBs is that their dispersion measures are very large and exceed the contribution from the electrons in our Galaxy by a factor of 10 — 20 in most cases. Lorimer et al. (2007) and Thornton et al. (2013) suggested that the large DM is dominated by the contribution from the ionized intergalactic medium (IGM). It implies that FRBs may occur at cosmological distances. With their large DMs, FRBs may be a powerful probe for studying the IGM and the spatial distribution of free electrons.

The millisecond duration of FRBs suggests that the sources should be compact, and the high radio brightness requires a coherent emission mechanism (Katz 2014a; Luan & Goldreich 2014). Since FRBs' redshifts are estimated to be in a range of $z \sim 0.5$ — 1.3 (Thornton et al. 2013; Champion et al. 2016) and FRB 150418 has been measured with a redshift $z = 0.492 \pm 0.008$ (Keane et al. 2016), the emitted energy at radio wavelengths can be as high as $\sim 10^{39}$ — 10^{40} ergs. Although the physical nature of FRBs is still unclear, some possible mechanisms have been proposed, such as double neutron stars (NS) merger (Totani 2013), interaction of planetary companions with the magnetic fields of pulsars (Mottez & Zarka 2014), collapses of hypermassive neutron stars into black holes (Falcke & Rezzolla 2014; Ravi & Lasky 2014; Zhang 2014), magnetar giant flares (Kulkarni et al. 2014; Lyubarsky 2014; Pen & Cornor 2015), supergiant pulses from pulsars (Cordes & Wasserman 2016), collisions of asteroids with NS (Geng & Huang 2015; Dai et al. 2016) or the inspiral of double NS (Wang et al. 2016). Keane et al. (2016) suggested that there may actually be more than one class of FRB progenitors.

People are eagerly hoping to detect much more FRBs in the near future. The event rate of FRBs and the observation power of our radio telescopes then become two major factors being involved. Thornton et al. (2013) have argued that if FRBs happens in the sky isotropically, their actual event rate could be as high as $\sim 10^4 \text{ sky}^{-1} \text{ day}^{-1}$. Hassall, Keane & Fender (2013) discussed the prospects of detecting FRBs with the next-generation radio telescopes and suggested that the Square Kilometer Array (SKA) could detect about one FRB per hour. Based on the redshifts estimated from the measured DMs, Bera et al. (2016) studied the FRB population and predicted that the upcoming Ooty Wide Field Array¹ can detect FRBs at a rate of ~ 0.01 — 10^3 per day, depending on the power-law index of the assumed distribution function, which could vary from -5 to 5. Note that their predicted detection rate is in a very wide range, which mainly stems from the large uncertainty of the FRB luminosity function.

The luminosities are strongly dependent on the measured redshifts. However, the redshifts of FRBs (except FRB 150418) are not directly measured, but are hinted from their DMs. The reliability of these redshifts still needs to be clarified (Katz 2014b; Luan & Goldreich 2014; Pen & Cornor 2015). In this study, we use the directly measured fluences of FRBs to derive an intensity distribution function. Our distribution function is independent of the redshift measurements. We then use the intensity distribution function to estimate the detection rate of FRBs by the Chinese Five-hundred-

metre Aperture Spherical radio Telescope (FAST) which is expected to begin operation in September 2016 (Nan et al. 2011). We also do some statistic researches on FRBs. Our article is organized as follows. In Section 2, we describe a sample of 16 non-repeating FRBs and present the statistical analyses of their parameters. In Section 3, we derive the intensity distribution function of FRBs. In Section 4, the observational prospects of FRBs with FAST are addressed. Our conclusions and discussion are presented in Section 5.

2 SAMPLES AND STATISTICAL ANALYSES

We extract the key parameters of 16 non-repeating FRBs detected by Parkes and GBT from the FRB Catalogue of Petroff et al. (2016)². The data are listed in Table 1. At the direction of FRB 121102, additional 16 repeating bursts were observed (Spitler et al. 2016; Scholz et al. 2016), indicating that all these events may be quite different from other non-repeating FRBs in nature. So we treat these 17 repeating events separately in our following study.

Column 1 of Table 1 provides the FRB names. The observed width or duration of the corresponding radio pulse (W_{obs}) is presented in Column 2. Column 3 is the observed peak flux density (S_{peak}) of each FRB. Columns 4 tabulates the observed fluences (F_{obs}) in units of Jy ms, which is calculated as $F_{\text{obs}} = S_{\text{peak}} \times W_{\text{obs}}$. Columns 5, 6, and 7 present the observed DMs of FRBs, the DM contributions from the Galaxy (DM_{Galaxy}), and the DM excesses (DM_{Excess}), respectively. The DM excess is defined as $DM_{\text{Excess}} = DM - DM_{\text{Galaxy}}$. The estimated redshift (z), the corresponding luminosity distances (D_L) and the emitted energies (E) are presented in Columns 8, 9, and 10, respectively.

We first focus on the distribution of the observed DMs of 16 non-repeating FRBs in Table 1. Fig. 1 illustrates the histogram of DMs (Panel a) and DM excesses (Panel b). Both DM and DM_{Excess} roughly follow the normal distribution and can be well fitted with a Gaussian function. The Gaussian function of DM peaks at 724 pc cm^{-3} with a dispersion of $\sigma_{DM} = 17 \text{ pc cm}^{-3}$, while DM_{Excess} peaks at $658 \pm 23 \text{ pc cm}^{-3}$. We see that $DM_{\text{Excess}}/DM \sim 90\%$, which supports the idea that FRBs may be of cosmological origin. Panel (c) of Fig. 1 shows that the estimated radio energy approximatively follows a log-normal distribution. The log-normal peak is about 10^{39} ergs, consistent with an earlier estimation by Huang & Geng (2016) when only 10 bursts were available.

In panel (a), (b) and (c) of Fig. 2, we plot the observed peak flux density, the observed fluence and the estimated radio energy against the DM excess, respectively. Fig. (2a) shows that S_{peak} does not have any clear correlation with DM_{Excess} , which is somewhat unexpected since a more distant source usually tends to be dimmer. One possible reason is that S_{peak} depends on the time and frequency resolution of the radio telescope, and another reason may be that the currently observed DM_{Excess} values are still in a relatively narrow range (the largest DM_{Excess} is only ~ 7 times that of the smallest one, and the estimated D_L range is a factor

¹ <http://rac.ncra.tifr.res.in/>

² <http://astronomy.swin.edu.au/pulsar/frbcat/>

Table 1. Key parameters of the 16 non-repeating FRBs. Observational data are mainly taken from <http://astronomy.swin.edu.au/pulsar/frbcat/> (Petroff et al. 2016).

FRB	W_{obs} (ms)	S_{peak} (Jy)	F_{obs} (Jy ms)	DM^a (pc cm^{-3})	DM_{Galaxy}^a (pc cm^{-3})	DM_{Excess}^b (pc cm^{-3})	z^c	D_{L}^c (Gpc)	E^c (10^{39} ergs)
(1)	(2)	(3)	(4)	(5)	(6)	(7)	(8)	(9)	(10)
010125	$10.60^{+2.80}_{-2.50}$	$0.54^{+0.11}_{-0.07}$	$5.72^{+2.99}_{-1.92}$	790.3 ± 0.3	110	680.3	0.57	3.35	2.77
010621	$8.00^{+4.00}_{-2.25}$	$0.53^{+0.26}_{-0.09}$	$4.24^{+5.24}_{-1.71}$	748 ± 3	523	223	0.19	0.93	0.12
010724	$20.00^{+0.00}_{-0.00}$	$1.57^{+0.00}_{-0.00}$	31.48	375 ± 3	44.58	330.42	0.28	1.45	2.31
090625	$1.92^{+0.83}_{-0.77}$	$1.14^{+0.42}_{-0.21}$	$2.19^{+2.10}_{-1.12}$	899.55 ± 0.1	31.69	867.86	0.72	4.46	2.42
110220	$5.60^{+0.10}_{-0.10}$	$1.30^{+0.00}_{-0.00}$	$7.28^{+0.13}_{-0.13}$	944.38 ± 0.05	34.77	909.61	0.76	4.77	9.39
110523	$1.73^{+0.17}_{-0.17}$	0.60	1.04	623.30 ± 0.06	43.52	579.78	0.48	2.73	0.22
110626	$1.41^{+1.22}_{-0.45}$	$0.63^{+1.22}_{-0.12}$	$0.89^{+3.98}_{-0.40}$	723.0 ± 0.3	47.76	675.54	0.56	3.28	0.48
110703	$3.90^{+2.24}_{-1.85}$	$0.45^{+0.28}_{-0.10}$	$1.76^{+2.73}_{-1.04}$	1103.6 ± 0.7	32.33	1071.27	0.89	5.80	3.59
120127	$1.21^{+0.64}_{-0.25}$	$0.62^{+0.35}_{-0.10}$	$0.75^{+1.04}_{-0.25}$	553.3 ± 0.3	31.82	521.48	0.43	2.39	0.20
121002	$5.44^{+3.50}_{-1.20}$	$0.43^{+0.33}_{-0.06}$	$2.34^{+4.46}_{-0.77}$	1629.18 ± 0.02	74.27	1554.91	1.30	9.28	14.94
130626	$1.98^{+1.20}_{-0.44}$	$0.74^{+0.49}_{-0.11}$	$1.47^{+2.45}_{-0.50}$	952.4 ± 0.1	66.87	885.53	0.74	4.62	1.75
130628	$0.64^{+0.13}_{-0.13}$	$1.91^{+0.29}_{-0.23}$	$1.22^{+0.47}_{-0.37}$	469.88 ± 0.01	52.58	417.3	0.35	1.87	0.19
130729	$15.61^{+9.98}_{-6.27}$	$0.22^{+0.17}_{-0.05}$	$3.43^{+6.55}_{-1.81}$	861 ± 2	31	830	0.69	4.24	3.35
131104	$2.37^{+0.89}_{-0.45}$	$1.16^{+0.35}_{-0.13}$	$2.75^{+2.17}_{-0.76}$	779 ± 3	71.1	707.9	0.59	3.50	1.72
140514	$2.80^{+3.50}_{-0.70}$	$0.47^{+0.11}_{-0.08}$	$1.32^{+2.34}_{-0.50}$	562.7 ± 0.6	34.9	527.8	0.44	2.46	0.37
150418	$0.80^{+0.30}_{-0.30}$	$2.20^{+0.60}_{-0.30}$	$1.76^{+1.32}_{-0.81}$	776.2 ± 0.5	188.5	587.7	0.49	2.79	0.66

^a DM and DM_{Galaxy} are the total dispersion measure and the contribution from the local Galaxy, respectively.

^b The dispersion measure excess, which is defined as $DM - DM_{\text{Galaxy}}$.

^c The redshifts are estimated from the corresponding DM excess. With these redshifts, the luminosity distances (D_{L}) and the emitted energies (E) can then be calculated.

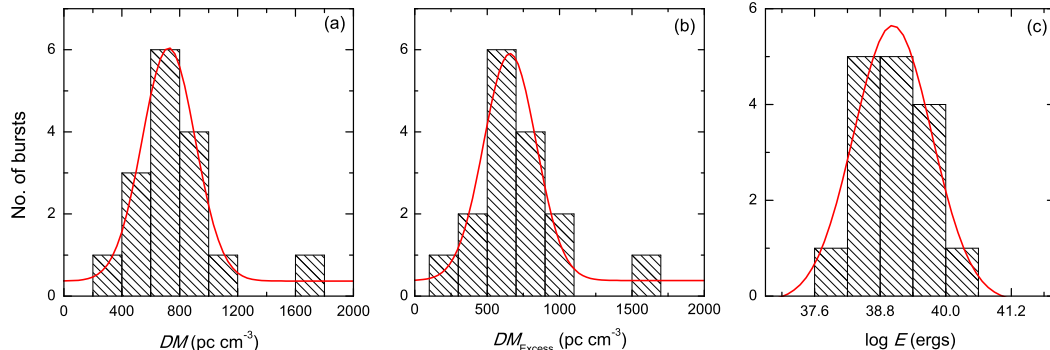


Figure 1. Distributions of the DM (Panel a), the DM excess (Panel b), and the estimated energy (Panel c). The solid curve in each panel is the best-fit Gaussian function, with the correlation coefficients and P-values being $(0.96, 4.76 \times 10^{-4})$, $(0.91, 7.39 \times 10^{-4})$ and $(0.95, 9.09 \times 10^{-6})$ in Panels (a), (b) and (c), respectively.

of ~ 10). Similarly, Fig. (2b) shows that F_{obs} does not correlate with DM_{Excess} . It indicates that the width of FRBs also does not depend on DM_{Excess} , which will be further shown in the following figures. In Fig. (2c), we see that the energies shows a strong correlation with DM_{Excess} , which is natural since the energy emitted has a square dependence on the distance. In fact, the best fit result of Fig. (2c) is $E \propto DM_{\text{Excess}}^{2.59 \pm 0.39}$, with the correlation coefficient and P-value (rejection possibility) as 0.78 and 1.07×10^{-5} , correspondingly. It corresponds to a correlation between the energy and the luminosity distance as $E \propto D_{\text{L}}^{2.05 \pm 0.32}$. The power-law index here is roughly consistent with the square relation, although with a still relatively large error box.

In Fig. (2d), we plot the observed peak flux density versus the observed pulse width, which shows the burst with a

stronger S_{peak} has a narrower W_{obs} . It is interesting to note that a similar tendency was found for giant pulses from some pulsars (e.g. Popov & Stappers 2007; Popov et al. 2009). Finally, we see that both E and DM_{Excess} do not correlate with W_{obs} (Figs. (2e) and (2f)). Note that while the observed pulse width is relatively clustered, the spread in the emitted energies is as large as three orders of magnitude. In panels (b) and (e), we marked the positions of FRBs 010621 and 010724. These two events seem to be quite different from others. We argue that they may form a distinct group, characterized by a low DM and a large fluence. It indicates that there may be at least two kinds of FRBs. More events detected in the future will help to clarify such a possibility.

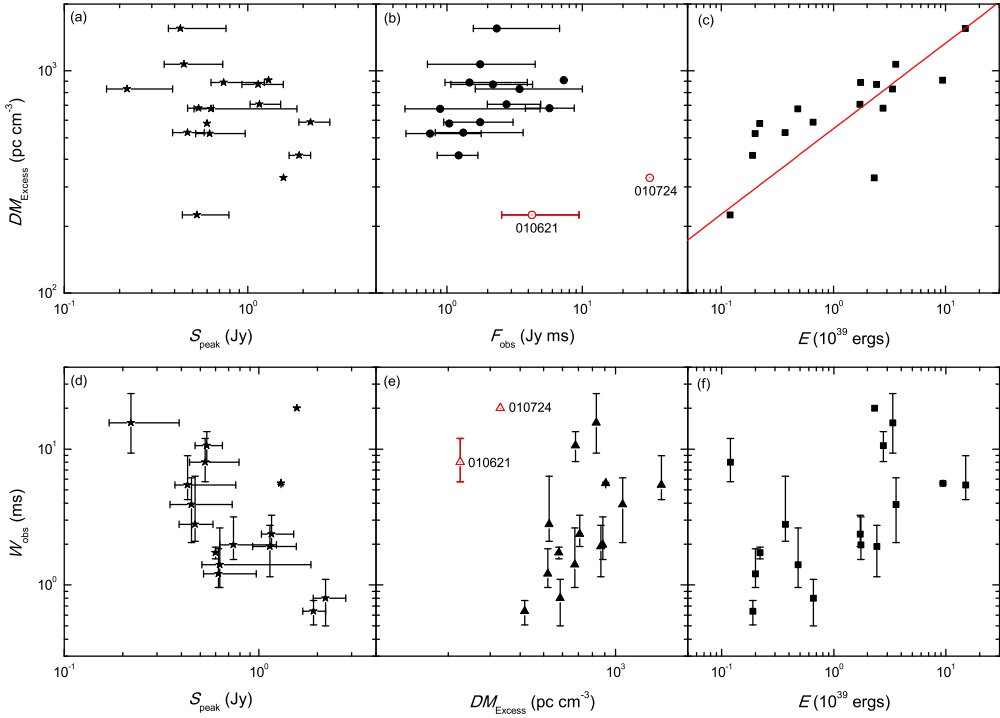


Figure 2. Panels (a), (b), and (c) illustrate the observed peak flux density (S_{peak}), the observed fluence (F_{obs}), and the estimated energy (E) against the DM excess (DM_{Excess}), respectively. Panels (d), (e) and (f) present S_{peak} , F_{obs} and E against the observed pulse width (W_{obs}), respectively. The best fit line is shown in Panel (c) when the two parameters are clearly correlated.

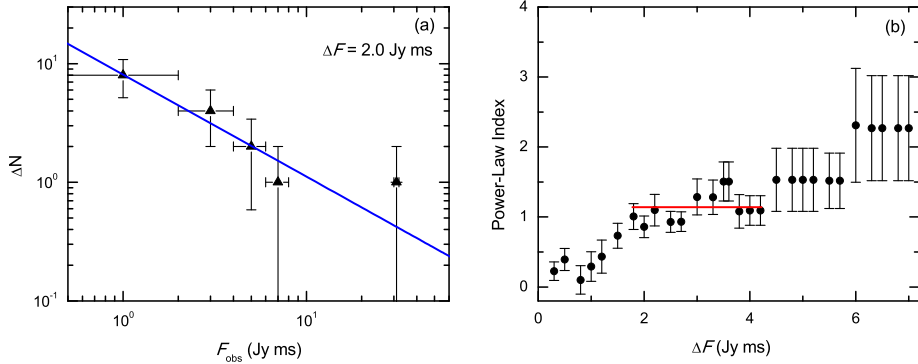


Figure 3. Intensity distribution functions of 16 non-repeating FRBs listed in Table 1 (Case I). The panel (a) shows an exemplar distribution function for a particular bin width, with the y -axis showing the number of FRBs in each bin. The panel (b) illustrates the best-fitted a values for different bin widths, in which the solid short horizontal line shows the average value of a for a preferable range of ΔF when a is relatively stable.

3 INTENSITY DISTRIBUTION FUNCTION

An absolutely scaled luminosity function can be helpful to address the nature of FRBs (Bera et al. 2016). However, since the redshifts of FRBs (except FRB 150418) have not been directly measured, the derived absolute luminosities and the emitted energies of FRBs are thus still controversial (Katz 2014b; Luan & Goldreich 2014; Pen & Connor 2015). On the other hand, the apparent intensity distribution function of astronomical objects can also provide helpful

information on their nature. A good example is the study of gamma-ray bursts (GRBs). Before 1997, when the redshifts of GRBs were still unavailable, a deviation from the $-3/2$ power-law function in the peak flux distribution of GRBs was noted (Tavani 1998). It was explained as a hint for the cosmological origin of GRBs, which was later proved by direct redshift measurements.

Here, we focus on the observed fluences (F_{obs}) of FRBs, but not simply the peak flux density. The reason is that radio sources can be seriously affected by scatter and scintillation

Table 2. The observable event rate of FRBs in the literature.

F_{Limit} (Jy ms)	$R(> F_{\text{Limit}})$ (sky $^{-1}$ day $^{-1}$)	Reference	Derived coefficient A (10 3 sky $^{-1}$ day $^{-1}$)
3.0	10 4	Thornton et al. (2013)	5.61 \pm 2.04
0.35	3.1 \times 10 4	Spitler et al. (2014)	7.88 \pm 6.92
2.0	2.5 \times 10 3	Keane & Petroff (2015)	1.17 \pm 0.51
1.8	1.2 \times 10 4	Law et al. (2015)	5.37 \pm 2.47
4.0	4.4 \times 10 3	Rane et al. (2016)	2.86 \pm 0.90
0.13-5.9	6.0 \times 10 3	Champion et al. (2016)	1.94 \pm 1.27

of IGM, which makes the peak flux density relatively unstable. The combination of F_{obs} and S_{peak} , i.e. the fluence, can then more reliably indicate the fierceness of FRBs. Another reason is that due to the limited time resolving power of our radio receivers, an FRB should last long enough to be recorded so that the duration is also a key factor. In fact, a tentative cumulative distribution vs. the fluence has been drawn by Katz (2016) based on a smaller data set constituted of 10 FRBs. Caleb et al. (2016a) has also tried to compose a cumulative $\log N(> F) - \log F$ correlation by using 9 FRBs in the high latitude (Hilat) region of Parkes survey.

We assume that the actual number density of FRBs occurring in the whole sky per day at a particular fluence F_{obs} follows a power-law function, i.e. $dN/dF_{\text{obs}} = A F_{\text{obs}}^{-a}$, where A is a constant coefficient and a is the power-law index. Both A and a need to be determined from observations. Note that A is in units of events sky $^{-1}$ day $^{-1}$. We first only consider the 16 non-repeating FRBs in Table 1 as the input data (Case I). We group the 16 FRBs into different fluence bins with a bin width of ΔF , count the number of FRBs in each bin and get the best-fitted power-law function for dN/dF_{obs} . In panel (a) of Fig. 3, we show the best-fitted result when the bin width is taken as $\Delta F = 2.0$ Jy ms. The fitted power-law index is $a = 0.86 \pm 0.15$, with the fitted correlation coefficient being 0.86 and the corresponding P-value being 0.001. Note that the error bars along x -axis simply represent the bin size, and the y -axis error bars are the statistical errors, which are the square root of the number in each bin.

Obviously, since the total number of FRBs is still very limited, the choice of the bin width will seriously affect the fitting result. So, we have tried various bin width ranging from 0.3 Jy ms to 7.0 Jy ms to study the effect. For these different bin widths, the derived power-law indices are illustrated in Panel (b) of Fig. 3. From this panel, we see that when the bin width is very small ($\Delta F \leq 1.8$ Jy ms), the fitted a value depends strongly on the bin width. The reason is that only two or three FRBs are grouped into one bin generally, thus the fluctuation dominates the final result. Meanwhile, when the bin width is too large ($\Delta F > 4.2$ Jy ms), the error bar of the fitted a also becomes larger. In these cases, only two or three bins are left with a non-zero number of FRBs so that the derived a becomes unreliable again. On the contrary, when ΔF is in the range of 1.8 — 4.2 Jy ms, the best-fitted a keeps to be somehow constant and the error box is also small. So we choose such a ΔF range to derive the a parameter. To reduce the effects of fluctuation as far as possible, we add up all the 12 a values derived for ΔF ranging between 1.8 Jy ms $\leq \Delta F \leq 4.2$ Jy ms to get a mean value for a (designated as a_1 for Case I), which finally gives $a_1 = 1.14 \pm 0.20$ (see Fig. (3b)).

Integrating the intensity distribution function, we can derive the FRB event rate above a particular fluence limit

in the whole sky per day as

$$R(> F_{\text{Limit}}) = A \int_{F_{\text{Limit}}}^{F_{\text{max}}} F_{\text{obs}}^{-a} dF_{\text{obs}}, \quad (1)$$

where F_{Limit} corresponds to the limiting sensitivity of a radio telescope, F_{max} is the upper limit of the fluence of observed FRBs, which is set as 35 Jy ms in our calculations (the observed maximum fluence is ~ 32 Jy ms at present). A is an unknown coefficient. It still needs to be determined from observations. FRBs were mainly identified from the archival data of several radio surveys. Constraints on the actual event rates of FRBs above a certain fluence limit were also derived in these analyses and were reported in the literature. We sum up these constraints in Table 2. According to Eq. (1), these data can be used to derive the coefficient A by using our best-fit a_1 value. The results are also listed in the last column in Table 2. Combining all these different A values, we finally get a mean value as $A = (4.14 \pm 1.30) \times 10^3$ sky $^{-1}$ day $^{-1}$. After getting the power-law index a and the constant coefficient A , we now can write down the full apparent intensity distribution function as,

$$\frac{dN}{dF_{\text{obs}}} = (4.14 \pm 1.30) \times 10^3 F_{\text{obs}}^{-1.14 \pm 0.20} \text{ sky}^{-1} \text{ day}^{-1}, \quad (2)$$

where F_{obs} is in units of Jy ms.

In total, 17 repeating FRB events have been detected from the source of FRB 121102. We treat these events as a separate group (Case II) and also study their intensity distribution. Similar fitting processes as for Case I are applied to Case II, the final results are shown in panel (a) and (b) of Fig. 4. In Fig. (4a), we show the exemplar fitting result when taking the bin width as $\Delta F = 0.32$ Jy ms. The best-fitted power-law index is 1.16 ± 0.06 , with the correlation coefficient and P-value being 0.99 and 0.001, respectively. Similar to Fig. (3b), Fig. (4b) shows the derived a values for different bin widths. The most probable mean value of a (designated as a_2 for Case II) is calculated for ΔF ranging between 0.2 Jy ms and 0.35 Jy ms, which is $a_2 = 1.03 \pm 0.16$.

Note that although a_1 and a_2 do not differ from each other markedly, there are actually significant differences between the overall characteristics of non-repeating FRBs and repeating FRBs. For example, the most obvious difference is that the repeating FRBs are generally weaker, indicating that they are mainly at the weak end of the fluence distribution. To show this tendency more clearly, we have combined all the FRBs in Cases I and II to form a third group (Case III). The total number of events is now 33. Similar plots for all the 33 FRBs are presented in Figs. (4c) and (4d). As shown in Fig. (4c), when the bin width is taken as 2.2 Jy ms, the power-law index is 1.81 ± 0.20 , with the correlation coefficient and P-value being 0.94 and 0.001, respectively. From Fig. (4d), the most probable mean value of a (designated as a_3 for Case III) is now derived as $a_3 = 1.95 \pm 0.29$ for the bin width ranging between $1.8 \text{ Jy ms} \leq \Delta F \leq 4.2 \text{ Jy ms}$. We see that a_3 is significantly larger than a_1 and a_2 , indicating that the intensities of the repeating bursts are generally lower than that of the non-repeating ones.

4 PROSPECTS FOR FAST

FAST (Nan et al. 2011; Li, Nan & Pan 2013), an ambitious Chinese megascience project, is currently being built in

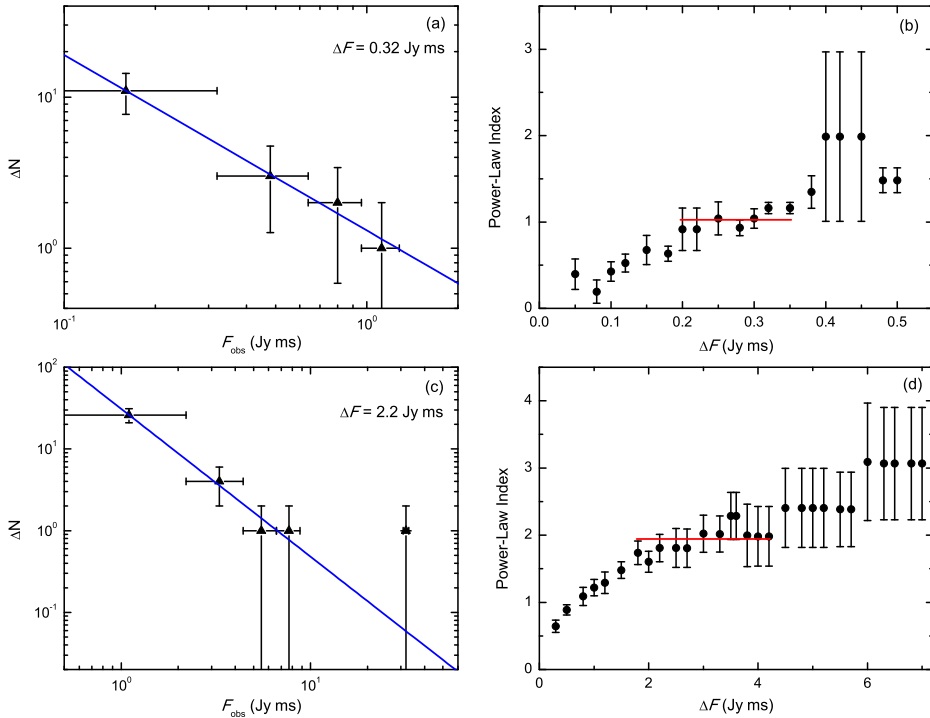


Figure 4. Intensity distribution functions of 17 repeating FRBs (Case II) and all the 33 detected FRBs (Case III). Panels (a) and (b) are plotted for 17 repeating FRBs from the source of FRB 121102. Panels (c) and (d) are plotted by combining all the 33 detections. Symbols are the same as Fig. 3.

Guizhou province in the southwestern of China. With a geometrical diameter of 500 meters and an effective diameter of ~ 300 meters at any particular moment, it will be the largest single-dish radio telescope in the world when it comes into operation in September of 2016. FAST's receivers will cover both low frequency (70-500 MHz) and middle frequency (0.5-3 GHz) bands. We here consider the prospect of detecting FRBs with FAST by using the derived intensity distribution function. Our calculations are done at the L band (1400 MHz) of FAST, which should be the most favorable wavelength for FRB observations.

The sensitivity or the limiting flux density (S_{limit}) of a radio telescope can be estimated as (Zhang et al. 2015),

$$S_{\text{limit}} \simeq (12\mu\text{Jy}) \left(\frac{0.77 \times 10^3 \text{m}^2/\text{K}}{A_e/T_{\text{sys}}} \right) \left(\frac{S/N}{3} \right) \left(\frac{1\text{hour}}{\Delta\tau} \right)^{1/2} \left(\frac{100\text{MHz}}{\Delta\nu} \right)^{1/2}, \quad (3)$$

where T_{sys} is the system temperature, $\Delta\tau$ is the integration time, $\Delta\nu$ is the bandwidth, S/N is the signal-to-noise ratio which is usually taken as 10 for a credible detection of a FRB (Champion et al. 2016), A_e is the effective area and it equals to $\eta_A \pi (d/2)^2$, with η_A being the aperture efficiency and d being the illuminated diameter. FAST has a system temperature of $T_{\text{sys}} \sim 25\text{K}$ at 1400 MHz. For other parameters of FAST, we take $d = 300\text{m}$, $\eta_A = 0.65$ (Zhang et al. 2015), $\Delta\nu = 300\text{ MHz}$, $\Delta\tau = 3\text{ ms}$ (Law et al. 2015). The limiting fluence of FAST is then calculated to be $F_{\text{Limit}} = S_{\text{limit}} \times \Delta\tau = 0.03\text{ Jy ms}$. Note that from Equations (1) and (2), the actual FRB event rate above the fluence limit of 0.03 Jy ms is $(3.03 \pm 1.56) \times 10^4 \text{ sky}^{-1} \text{ day}^{-1}$.

The beam size of a radio telescope is $\Omega \sim \pi\theta^2$, where $\theta \sim 1.22(\lambda/d)$ is the half opening angle of the beam. For FAST, the beam size is $\Omega \sim 0.008 \text{ deg}^2$ at 1400 MHz. FAST's receiver has 19 beams in L band, and the corresponding total instantaneous field-of-view (FoV) is 0.15 deg^2 . Considering Eq. (2) and all these parameters, we can get the daily detection rate of FRBs by FAST as,

$$R_{\text{FAST}} \sim (3.03 \pm 1.56) \times 10^4 \times \frac{0.15 \text{ deg}^2}{41253 \text{ deg}^2} \text{ day}^{-1} \quad (4) \\ = 0.11 \pm 0.06 \text{ day}^{-1}.$$

For a 1000 hours of observation time, this will correspond to $\sim 5 \pm 2$ detections. Parkes telescope has an FoV of 0.55 deg^2 and a sensitivity of 0.05 Jy . In the Parkes Hילat survey, 9 FRBs have been identified, which suggests a rate of $R_{\text{Parkes}} = 0.08 \pm 0.03 \text{ events day}^{-1}$ (Thornton et al. 2013; Champion et al. 2016; Caleb et al. 2016b). The FRB detection rate of FAST against Parkes will be $\sim 0.11/0.08 \sim 1.5$, which is quite reasonable.

5 DISCUSSION AND CONCLUSIONS

In this study, we analyse statistically the key parameters of the 16 non-repeating FRBs detected by Parkes and GBT. The observed DM spans a range of $375 - 1629 \text{ pc cm}^{-3}$ and peaks at $\sim 724 \text{ pc cm}^{-3}$, while the DM excess peaks at $\sim 658 \text{ pc cm}^{-3}$ and typically accounts for $\sim 90\%$ of the total DM. The emitted radio energy spans about three orders of magnitude, with the mean energy being about 10^{39} ergs . While most of the parameters do not correlate

with each other, a burst with stronger S_{peak} tends to have shorter duration, and a clear correlation between the radio energy released and the DM excess has been found to be $E \propto DM_{\text{Excess}}^{2.59 \pm 0.39}$ (Fig. 2c), which may reflect the square dependence of the emitted energy on the distance. From these statistical analyses, we found that FRBs 010621 and 010724 are quite different from others and they may form a distinct group.

Using the observed fluence as an indication for the strength of FRBs and combining the constraints on the event rate of FRBs from various observational surveys, we derived an apparent intensity distribution function for the 16 non-repeating FRBs as $dN/dF_{\text{obs}} = (4.14 \pm 1.30) \times 10^3 F_{\text{obs}}^{-1.14 \pm 0.20} \text{ sky}^{-1} \text{ day}^{-1}$. For FRB 121102 and its repeating bursts, the corresponding power-law index is derived to be $a_2 = 1.03 \pm 0.16$, and for all the 33 detections, the power-law index is $a_3 = 1.95 \pm 0.29$. Based on the intensity distribution function, we were able to estimate the detection rate of FRBs by China's coming FAST telescope. With a sensitivity of 0.03 Jy ms and a total instantaneous FoV of 0.15 deg² (19 beams), FAST will be able to detect roughly 1 FRB for every 10 days of observations, or about 5 events for every 1000 hours.

A few authors have studied the cumulative distribution function of FRBs (Bera et al. 2016; Caleb et al. 2016a; Katz 2016; Wang & Hu 2016), which is usually assumed to be a power-law function of $N_{>F_{\text{obs}}} \propto F_{\text{obs}}^{-\alpha}$. For standard candles distributed homogeneously in a flat Euclidean space, the value of α should be 3/2 (Thornton et al. 2013). Oppermann, Connor & Pen (2016) has argued that the range of α may be $0.9 \leq \alpha \leq 1.8$, Caleb et al. (2016a) has derived $\alpha = 0.9$ for a small sample of 9 Hilat FRBs, while Wang & Hu (2016) considered α as 0.78 for FRB 121102 and 16 repeating bursts. Note that the relation between cumulative index α and our intensity distribution index a is $\alpha = a - 1$. So, our derived index of $a = 1.14 \pm 0.20$ will correspond to $\alpha = 0.14 \pm 0.20$. It is significantly smaller than Caleb et al.'s value. The difference could be caused by different sample capacity. We have 16 non-repeating FRBs in our sample. However, when we include all the repeating and non-repeating FRBs in our study, the derived index is $a_3 = 1.95 \pm 0.29$, which corresponds to $\alpha = 0.95 \pm 0.29$ and will be comparable to that of Caleb et al.'s. But even in this case, the α index is still markedly smaller than 3/2. It strongly points toward a deficiency of the dimmest FRBs, which has also been indicated in earlier studies (Bera et al. 2016; Caleb et al. 2016a; Katz 2016; Lyutikov, Burzawa & Popov 2016). There are a few factors that could lead to such a deviation. First, the total number of currently observed FRBs is still very limited. It can result in a large fluctuation in the measured power-law index. In fact, Caleb et al. (2016a) have estimated that at least ~ 50 FRBs are needed to extract conclusive information on the physical nature of FRBs. Second, FRBs are not ideal standard candles, their brightness has been found to distribute in a relatively wide range. But as long as the characteristics of FRBs does not evolve systematically with the distance, the index will not be affected too much. A wider brightness range will only result in a larger error box for α , which can still be reduced by increasing the FRB samples. Third, FRBs may not be homogeneous sources, the co-moving density or their brightness may evolve in space. For example, the co-moving FRB den-

sity may be smaller when the distance increases, or farther FRBs may not be as fierce as those nearer to us. Fourth, the space may not be a flat Euclidean space, such as for a curved Λ -CDM cosmology. In this case, the deviation of α from 3/2 can be used as a probe for the cosmology (Caleb et al. 2016a). Finally, it should also be noted that the apparent deficiency of the dimmest FRBs could also be due to the selection effect. Much weaker FRB events may actually have happened in the sky, but we were not able to record them or find them due to current technical limitations. To make clear which of the above factors has led to the smaller α , more new FRB samples would be necessary in the future.

As addressed above, the apparent intensity distribution function derived here is still a preliminary result. We need much more samples to determine the power-law index more accurately. With an enormous effective area for collecting radio emissions, the Chinese FAST telescope is very suitable for FRB observations. It may be able to increase the FRB samples at a rate of ~ 10 events per year (assuming an effective observation time of 2000 hours). More importantly, FAST can operate in a very wide frequency range and can hopefully provide detailed spectrum information for FRBs. It is expected to be a powerful tool in the field.

At present, whether FRBs are beamed or not is still an unclear but important problem. If FRBs are highly collimated, the actual energy released will be much smaller than the currently estimated energy base on an assumed solid angle of ~ 1 sr (Huang & Geng 2016). The emission mechanisms of FRBs will then involve complex jet effects (Borra 2013). Studying the jet effects of FRBs will be an important task and it will help us understand explosion mechanisms of FRBs. When more FRBs are observed and localized, we may be able to get useful information on beaming effects from direct observations.

ACKNOWLEDGMENTS

This study was supported by the China Ministry of Science and Technology under State Key Development Program for Basic Research (973 program, Grant Nos. 2014CB845800, 2012CB821802), the National Natural Science Foundation of China (Grant Nos. 11473012, U1431126, 11263002) and the Strategic Priority Research Program (Grant No. XDB09010302).

REFERENCES

- Bera A., Bhattacharyya S., Bharadwaj S., Bhat N. D. R., Chengalur, J. N., 2016, MNRAS, 457, 2530
- Borra E. F., 2013, ApJ, 774, 142
- Burke-Spolaor S., Bannister K. W., 2014, ApJ, 792, 19
- Caleb M., Flynn C., Bailes M., Barr E. D., Hunstead R. W., Keane E. F., Ravi V., van Stratenet W., 2016, MNRAS, 458, 708
- Caleb M. et al., 2016, MNRAS, 458, 718
- Champion D. J. et al., 2016, MNRAS, submitted (arXiv:1511.07746)
- Cordes J. M., Wasserman I., 2016, MNRAS, 457, 232
- Dai Z. G., Wang J. S., Wu X. F., Huang Y. F., 2016, preprint (arXiv:1603.08207)

Falcke H., Rezzolla L., 2014, *A&A*, 562, A137

Geng J. J., Huang Y. F., 2015, *ApJ*, 809, 24

Gu W. M., Dong Y. Z., Liu T., Ma R., Wang J. F., 2016, preprint(arXiv.1604.05336)

Hassall T. E., Keane E. F., Fender R. P., 2013, *MNRAS*, 436, 371

Huang Y. F., Geng J. J., 2016, in Proceedings of “Frontiers in Radio Astronomy and FAST Early Sciences Symposium 2015 (FRA 2015)”, conference hold in Guiyang, China in July 2015, Astronomical Society of the Pacific, 502, 1

Katz J. I., 2014a, *Phys. Rev. D*, 89, 103009

Katz J. I. 2014b, preprint (arXiv:1409.5766)

Katz J. I., 2016, *ApJ*, 818, 19

Keane E. F., Petroff E., 2015, *MNRAS*, 447, 2852

Keane E. F., Stappers B. W., Kramer M., Lyne A. G., 2012, *MNRAS*, 425, L71

Keane E. F. et al., 2016, *Nature*, 530, 453

Kulkarni S. R., Ofek E. O., Neill J. D., Zheng Z., Juric M., 2014, *ApJ*, 797, 70

Law C. J. et al., 2015, *ApJ*, 807, 16

Li D., Nan R., Pan Z., 2013, in IAU Symposium Vol. 291 of IAU Symposium, The Five-hundred-meter Aperture Spherical radio Telescope project and its early science opportunities. pp 325–330

Lorimer D. R., Bailes M., McLaughlin M. A., Narkevic D. J., Crawford F., 2007, *Science*, 318, 777

Luan J., Goldreich P., 2014, *ApJ*, 785, L26

Lyubarsky Y., 2014, *MNRAS*, 442, L9

Lyutikov M., Burzawa L., Popov S. B., 2016, preprint (arXiv:1603.02891)

Mottez F., Zarka P., 2014, *A&A*, 569, A86

Masui K. et al., 2015, *Nature*, 528, 523

Nan R. D. et al., 2011, *Int. J. Mod. Phys. D*, 20, 989

Oppermann N., Connor L., Pen U.-L., 2016, preprint (arXiv:1604.03909)

Pen U.-L., Connor L., 2015, *ApJ*, 807, 179

Petroff E. et al., 2015a, *MNRAS*, 447, 246

Petroff E. et al., 2015b, *MNRAS*, 454, 457

Petroff E. et al., 2016, preprint (arXiv:1601.03547)

Popov M. V., Stappers B., 2007, *A&A*, 470, 1003

Popov M. et al., 2009, *PASJ*, 61, 1197

Rane, A., Lorimer, D. R., Bates, S. D., McMann N., McLaughlin M. A., Rajwade K., 2016, *MNRAS*, 455, 2207

Ravi V., Lasky P. D., 2014, *MNRAS*, 441, 2433

Ravi V., Shannon R. M., Jameson A., 2015, *ApJ*, 799, L5

Scholz P. et al., 2016, preprint (arXiv:1603.08880)

Spitler L. G. et al., 2014, *ApJ*, 790, 101

Spitler L. G. et al., 2016, *Nature*, 531, 202

Thornton D. et al., 2013, *Science*, 341, 53

Totani T., 2013, *PASJ*, 65, L12

Wang F. Y., Yu H., 2016, preprint (arXiv: 1604.08676)

Wang J. S. Yang Y. P., Wu X. F., Dai Z. G., Wang F. Y., 2016, *ApJ*, 822, L7

Zhang B., 2014, *ApJ*, 780, L21

Zhang Z. B., Kong S. W., Huang Y. F., Li D., Li L. B., 2015, *Res. Astron. Astrophys.*, 15, 237